Challenges and Applications of Registering 3D Ultrasound Computer Tomography with Conventional Breast Imaging Techniques

P. Cotic Smole[1], N.V. Ruiter[1], N. Duric[2], and T. Hopp[1]

[1]*Karlsruhe Institute of Technology, Institute for Data Processing and Electronics, Karlsruhe, Germany*
E-mail: patricia.smole@kit.edu, torsten.hopp@kit.edu
[2]*Barbara Ann Karmanos Cancer Institute, Department of Oncology, Detroit, USA*

Abstract

To evaluate the diagnostic value of Ultrasound Computer Tomography (USCT), the imaging results have to be correlated with conventional breast imaging techniques. This is challenging due to different patient positioning in the modalities with nonlinear deformations of the breast tissue. We have developed a patient-specific image registration method, which simulates different breast positionings in both X-ray mammography and Magnetic Resonance Imaging (MRI) through biomechanical modelling. An average registration error below 5 and 17 mm for MRI to USCT and USCT to mammography registration, respectively, allowed us to evaluate the diagnostic performance of USCT. It was shown that regions of high sound speed corresponded well with the tumour position indicated from the MRI contrast kinetic map. Moreover, the quantitative analysis of sound speed and attenuation values with respect to the segmented mammograms revealed that sound speed gives a better distinction between breast tissue, whereas their combined information further improves the classification. Although the results are based on a preliminary study, the promising outcome points that the registration could assist radiologists in comparing the USCT with both MRI and X-ray mammography.

Keywords: Breast image registration, Ultrasound computer tomography, X-ray mammography, Magnetic resonance imaging, Multimodal diagnosis

1   Introduction

3D Ultrasound Computer Tomography (USCT) is a promising imaging method for breast cancer diagnosis that is currently undergoing first evaluations in clinical trials [1, 2, 3]. The method aims to provide high resolution 3D images of the undeformed breast by using ultrasonic waves,

thereby enabling patient-friendly conditions. For image acquisition, more than two thousands ultrasound transducers surround the breast in a water bath. The transducers emit unfocussed ultrasound waves and record the reflected and transmitted signals that are generated upon interaction of the wave with the breast tissue. A single image acquisition allows the reconstruction of three tissue characteristics: reflectivity, sound speed and attenuation. While reflectivity images visualize the tissue boundaries, sound speed and attenuation images provide quantitative tissue characterization [4].

In the current development state, it is essential to correlate USCT images to conventional imaging modalities to evaluate its diagnostic value and further improve the data acquisition and image reconstruction process. Besides the screening modality X-ray mammography, magnetic resonance imaging (MRI) is frequently used for early breast cancer diagnosis. To directly compare USCT with both modalities, the challenge is to overcome the substantial differences in patient positioning and breast deformation in order to provide a spatial correspondence between images. Another obstacle is the different dimensionality of images (3D USCT vs. 2D mammograms).

In this paper, we present a patient-specific image registration method that estimates the spatial transformation between images, governed by the differences between imaging modalities. Patient-positioning conditions and breast deformations are simulated by employing biomechanical modelling and an X-ray like projection of the USCT volume is used to enable a comparison with 2D mammograms. We give a review of its recent developments, present the first evaluation results of USCT's diagnostic value and raise open challenges.

2   Methods

The aim of the registration approach is to spatially align the breast shape observed in one modality (source image) as good as possible with the shape observed in the compared modality (target image). With a biomechanically-based registration we aim in modelling the different conditions in patient-positioning and breast deformation of imaging modalities:

- USCT: breast in prone position, immersed in water;

- X-ray mammography: breast in upright position, compressed between parallel plates;

- MRI: breast in prone position, placed within MRI breast coils.

Hence, the following loading conditions are simulated for the registration of MRI to USCT respectively USCT to X-ray mammography:

- MRI to USCT: the buoyancy effect is simulated on the MRI volume to estimate the approximate gravity-free state of the breast observed in USCT;

- USCT to X-ray mammography: the breast compression is simulated on the USCT volume to mimic the mammographic compression.

In the following, a detail description of the breast image registration workflow is presented.

2.1 Breast image registration

The registration approach is based on the biomechanical modelling used in the registration of MRI with X-ray mammography [5]. The model is generated from the MRI volume (MRI-USCT registration) respectively USCT volume (USCT-mammography registration). To estimate the breast stiffness distribution for MRI to USCT registration, the MRI volume is segmented into background, fatty and glandular breast tissues using unsupervised fuzzy c-means algorithm [6] and Level-Set-Evolution [7]. Young's moduli of fatty (E_{fat}) and glandular tissue (E_{gland}) are initially applied constant for all patients and are subsequently updated by a patient-specific parameter optimization. Initial E_{fat} and E_{gland} are in the range of experimental values in literature [8]: $E_{fat} = 900\,\text{Pa}$ and $E_{gland} = 1200\,\text{Pa}$. The segmented MRI volume is further cropped at the sternum in anteroposterior direction to take into account only the relevant part of the breast for the registration with USCT.

For USCT to X-ray mammography registration, a patient-specific stiffness distribution model is constructed from the preprocessed USCT sound speed image that provides a voxel-based model. The motivation for using a voxel-based stiffness distribution is two fold. First, automated segmentation of breast tissue types in USCT images is challenging and not yet developed. Second, due to the physical relationship between the sound speed and elastic properties of tissue, the Young's modulus E can be estimated for each voxel from the sound speed map.

The geometry of the segmented MRI volume respectively USCT sound speed image is generated by a volumetric meshing algorithm [9] using 4-node tetrahedrons. A hyperelastic neo-hookean material model is used. The neo-hookean material constants are computed based on the relationship between the Young's modulus and the shear and bulk modulus as described in e.g. Bower [10]. A Poisson ratio close to 0.5 assumes the breast tissue to be nearly incompressible.

For both MRI to USCT and USCT to X-ray mammography registration, the simulation of different loading conditions is implemented using the commercial Finite Element Methods (FEM) software ABAQUS [11]. For MRI to USCT registration, the buoyancy effect is simulated by applying a body load $F = \rho V g$, where ρ refers to the density of water, V to the volume of the water displaced by the breast and g is the gravitational acceleration factor in anteroposterior direction. In the case of USCT to X-ray mammography registration, the mammographic compression of the breast is modelled by a displacement-driven movement of two parallel plates in the craniocaudal direction until a compression thickness retrieved from the mammogram's metadata is achieved. The deformation of the breast is governed by a contact definition between the plates and the breast. During both simulation strategies, the posterior-most nodes

are kept in position to model the fixation of the breast at the chest wall. For the comparison of the USCT volume with the 2D mammograms, a maximum intensity projection is additionally derived from the deformed USCT volume.

The presented registration process is based on several preprocessing parameters that govern the biomechanical model creation and simulation. To adapt the process to patient-specific conditions, we allow the optimization of the most influencing patient-specific parameters with respect to maximizing the image similarity between the deformed source image and target image. We focused on optimizing the following parameters: the rotation around the anteroposterior direction that accounts for any relative rotation and tilting of the patient between both modalities (MRI-USCT, USCT-X ray mammography), the cropping position of the MRI volume in anteroposterior direction (MRI-USCT), the Young's moduli of fatty and glandular tissue (MRI-USCT). The image similarity is calculated based on the surface agreement between the deformed MRI volume and the USCT volume, respectively gradient correlation between the projection of the deformed USCT volume and the 2D mammogram. The optimization is implemented using the simulated annealing algorithm [12] with a stopping condition of 100 iterations.

In addition to the biomechanically-based registration, both registration approaches underwent an additional surface-based registration that directly matches the volume surface of the source to the target image, thereby enabling direct comparison of imaging modalities. In the case of USCT to X-ray mammography registration, the 3D profile of the breast was approximated by a semi-ellipsoidal shape, where the projection of the breast boundary was extracted from the mammogram and the height matched the compression thickness given from the mammogram's meta data. The use of this second registration step aimed to overcome the uncertainties and simplifications made in biomechanical modelling such as neglecting tissue structures like Cooper ligaments or neglecting breast deformations caused by the MRI breast coils.

The outcome of the registration approach is a registered breast volume of the source image that directly matches the volume in the target image. A workflow of the registration approach is schematically depicted in figure 1 for the example of USCT to X-ray mammography registration. A detail description of the whole registration is beyond the scope of this paper and can be found in [13, 14].

2.2   Evaluation method

To evaluate the approach for MRI to USCT registration, nine datasets from a clinical study performed at the University Hospital Jena were used, whereas USCT to X-ray mammography registration was evaluated from nine datasets acquired at the Karmanos Cancer Institute. Each consisted of volume images of the three USCT image types (reflectivity, attenuation and sound speed), as well as the corresponding T1-weighted MRI volume respectively craniocaudal mammogram. The registration accuracy was measured based on landmarks such as lesions, predominant connective tissue structures or breast implants that could be clearly delineated in

both compared modalities. The borders of the landmarks were manually annotated by using a freehand tool. In the case of USCT to X-ray mammography, the target registration error (TRE) was calculated as the 2D Euclidean distance between the centre positions of the annotation in the projection of the deformed USCT volume and mammogram, whereas the average closest distance between pairs of annotation points in the deformed USCT volume and the MRI volume served for calculating the 3D TRE for USCT to MRI registration. Note that the different calculation approach of TRE arises as both studies were performed independently.
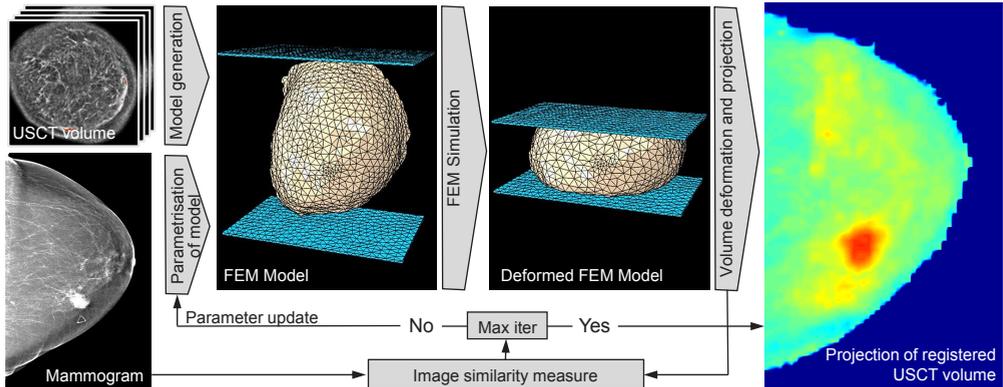
Figure 1: Schematic workflow presentation of the biomechanically-based image registration of USCT with X-ray mammography.

3 Results

3.1 Registration accuracy

For the analysed preliminary datasets, the presented registration approach showed to improve the registration accuracy by more than a factor of two compared to rigid alignment of the volumes at their centres of mass (table 1). As evident from the table, the mean TRE for USCT to X-ray mammography is more than three times larger than the TRE reached for MRI to USCT registration (16.2 mm vs. 4.7 mm) and has a much larger variance (9.0 mm vs. 1.7 mm). On one hand, this could be explained by the fact that the compression simulation induces much larger nonlinear deformations of the soft breast tissue compared to the buoyancy simulation and is as such more sensitive to uncertainties and simplifications in the breast modelling. On the other hand, differences in TRE could also arise as both registration strategies did not employ a common calculation approach for TRE.

(a) Patient with a breast implant   (b) Healthy patient
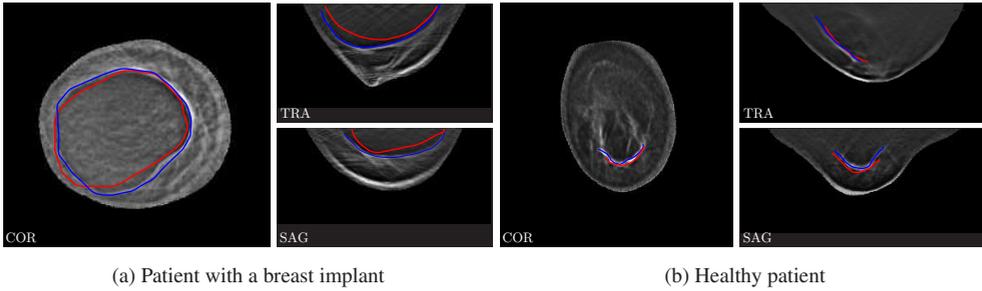
Figure 2: Resulting images of two patients for MRI to USCT registration. An overlap of the registered MRI annotation (red) and USCT annotation (blue) on the coronal (COR), sagittal (SAG) and transversal (TRA) USCT reflectivity slices. (a) A patient with a breast implant, (b) a healthy patient showing a high intensity connective tissue structure. Figures acquired from [14].

Figure 2 shows the resulting images of two patients for MRI to USCT registration, where the registered MRI annotation contour (red) is overlapped together with the USCT annotation contour (blue) on the USCT reflectivity image. The presented cases refer to a patient with a breast implant (figure 2a) and a healthy patient with a clearly visible connective tissue structure (figure 2b). In both cases, the annotations are well overlapping and can be delineated in the same slice in both modalities. The average TRE for these cases was 3.6 mm and 1.9 mm respectively.

3.2   Evaluation of USCT diagnostic value with MRI

In comparing USCT with MRI, we focused in assessing the diagnostic value of USCT for tumour detection by qualitative evaluation of USCT sound speed images with respect to the MRI contrast kinetic. The MRI contrast kinetic is a commonly used method to visualize tumours in contrast enhanced MRI and is based on monitoring the contrast agent uptake and washout over time through so called parametric maps, in which the three time point (3TP) method [15] is applied. The image intensity is evaluated at three time points: before, shortly after and approximately 6 to 7 minutes after the contrast agent was applied. For each voxel, both the contrast agent uptake between the first and second time point, as well as the wash out between the second and third time point are categorized into three intensity classes each. The washout categories are color-coded in red, green and blue and are together with the uptake-related brightness categories overlaid on the native MRI.

Biomechanical registration	$\mu_{\text{TRE}} \pm \sigma_{\text{TRE}}$	$TRE_{\text{Reg}}/\text{TRE}_{\text{Rigid}}$
MRI-USCT	4.7 ± 1.7 mm	2.2
USCT-Mammography	16.2 ± 9.0 mm	2.5

Table 1: Summary of mean target registration error (μ_{TRE}), standard deviation (σ_{TRE}) and ratio between mean TRE obtained from biomechanical image registration and mean TRE obtained from mere rigid alignment of volumes ($TRE_{\text{Reg}}/\text{TRE}_{\text{Rigid}}$).
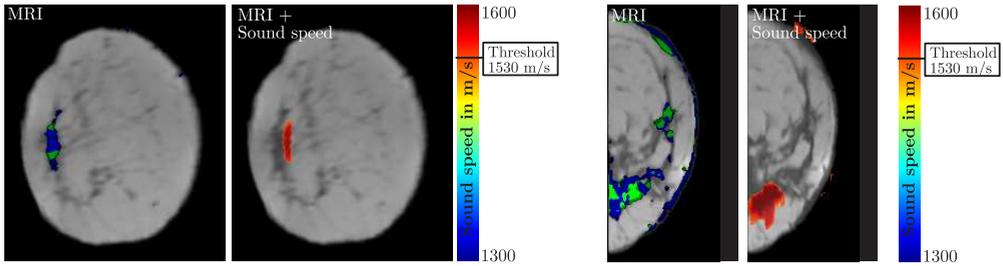
Figure 3: Comparison of registered native MRI with color-coded contrast kinetic analysis by the 3TP method (left subimage for each patient) and fused image from registered native MRI background and color-coded thresholded USCT sound speed (right subimage for each patient) for two patients (left and right image). Regions of high sound speed (red) correspond well with the tumour position in MRI indicated from the contrast kinetic as strong contrast agent uptake and a persistent respectively strong washout (green and blue). Figures acquired from [14].

A qualitative comparison of USCT and MRI for tumour detection is shown in figure 3 for two patients in terms of image fusion. Here, the USCT sound speed is presented as color-coded overlay on the MRI native grey-scale background in comparison to the MRI contrast kinetic analysis. From the fused images from USCT sound speed and native MRI, an area of high sound speed can be detected at approximately the same position, where the high contrast agent uptake and persistent respectively strong washout in the MRI refers to a detected tumour. This qualitative comparison of both modalities depicts that the registration is accurate enough for performing image fusion and that USCT sound speed may have a comparable diagnostic value for tumour detection as MRI contrast kinetic analysis.

3.3 Evaluation of USCT diagnostic value with X-ray mammography

Besides qualitatively evaluating the diagnostic value of USCT sound speed for the detection of tumours, the interest is to analyse whether a quantitative characterization of different tissue types is possible based on both the attenuation and sound speed values. We performed this analysis based on the registered USCT and X-ray mammography images. As a ground truth for the different tissue types, the mammogram was segmented into fatty, glandular and tumorous tissue using interactive thresholding and morphological closing, whereas the lesion was manually annotated. By comparing the projections of the registered sound speed and attenuation images to the mammogram, the segmentation served as a tissue mask to evaluate the average sound speed and attenuation values in fatty, glandular and tumorous tissue for each of the patients. To evaluate how well the average sound speed and attenuation values can separate different tissue types, a classification was further performed using a linear support vector machine (SVM) algorithm [16]. We used both the average sound speed and attenuation values obtained for each patient as features for a 3-class problem aiming in separating fatty, glandular and tumorous tissue. In a repeating process for all combinations of training-test-partitions, eight patient datasets were used in the training, whereas one dataset remained for testing.
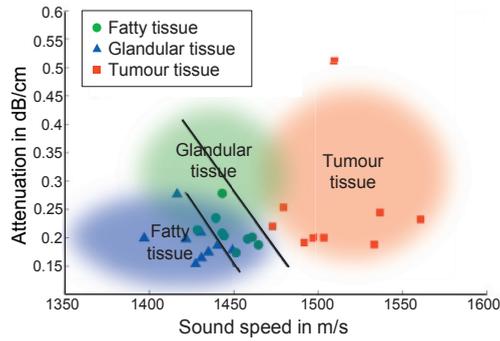
Figure 4: A scatter plot of average sound speed and attenuation values for fatty, glandular and tumorous tissue types for each patient in combination with the two tissue separation lines as obtained from SVM for the 3-class problem. The three transparent color clouds show approximately the expected tissue classification as obtained from Greenleaf et al. [4].

Figure 4 shows a scatter plot of average sound speed and attenuation values for fatty, glandular and tumorous tissue types for each patient in combination with the tissue separation lines as obtained from SVM for the 3-class problem. The training and test errors were 13% respectively 15%. As evident from the figure, the high error appeared due to hard separation between fatty and glandular tissue. That was also supported by a 2-class problem, where both the training and testing error were 0% in separating the fatty and glandular part from the tumorous part.

To present the fused information of both mammograms and projections of USCT sound speed, figure 5 presents an example where the tissue-characteristic sound speed is shown as a color-coded overlay on the grey-scale mammogram background. The different tissue regions in the sound speed image are separated based on the SVM classification output.
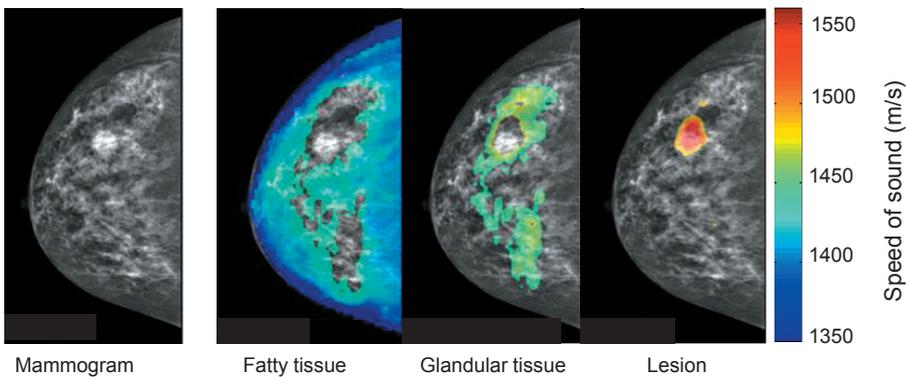
Figure 5: Image fusion of USCT sound speed projection and mammography. A color-coded overlay of tissue-specific sound speed values is shown on the grey-scale mammogram background. The different tissue regions in the sound speed image are separated based on the SVM classification.

4 Summary and Conclusion

We have developed and implemented a fully automated biomechanically-based image registration approach that matches the USCT reflectivity, sound speed and attenuation images with both MRI and X-ray mammography. By optimizing a set of the most influencing parameters, we enable a patient-specific registration. The evaluation with a preliminary dataset showed that the registration approach improves the registration accuracy by more than a factor of two in comparison to rigid alignment of the volumes at their centres of the mass. The average achieved target registration error for USCT to MRI matching was smaller than 5 mm, whereas an average accuracy of 16.2 mm was reached for USCT to X-ray mammography.

The achieved registration accuracy enabled us to evaluate the diagnostic performance of USCT with respect to both modalities. In visually comparing the USCT sound speed image to the registered MRI contrast kinetic map that depicts lesions, areas of high sound speed appeared to match approximately the same lesion region as detected from the contrast kinetic map. Moreover, quantitative evaluation of the average sound speed and attenuation values for different tissue types revealed that automatic classification of fatty, glandular and tumorous tissue may be possible and is more accurate when both image modalities are taken into account.

The presented method and its evaluation showed promising results in registering and fusing information from USCT with two different modalities with significant differences in patient positioning and breast deformation. Although the results were derived from a preliminary dataset, the approach clearly depicts that a direct correlation of tissue structures from different modalities may be possible. Therefore, it is likely to help assisting radiologists in the time consuming and challenging multimodal diagnosis of USCT data.

The presented biomechanical model was subjected to several uncertainties and simplifications in the modelling, which were overcome with a second surface-based registration. In order to omit this step, we plan to further extend the model by simulating tissue structures like Cooper ligaments, the breast-muscle interface, as well as pre-deformations of the breast caused by the MRI breast coils. In addition, we plan to investigate several registration strategies, such as the accuracy achieved in registering MRI to USCT in comparison to USCT to MRI, as well as the effect of the three-modal registration compared to the two-modal. Finally, additional approaches to evaluate the quantitative information of USCT images will be tackled.

References

[1] N.V. Ruiter, M. Zapf, R. Dapp, T. Hopp, W.A Kaiser, H. Gemmeke: First results of a clinical study with 3D ultrasound computer tomography. In: Ultrasonics Symposium (IUS), 2013 IEEE International, 651-654.

[2] N. Duric, P. Littrup: Clinical breast imaging with ultrasound tomography: A description of the SoftVue system. The Journal of the Acoustical Society of America 135(4) (2014) 2155.

[3] T. Hopp, M. Zapf, E. Kretzek, J. Henrich, A. Tukalo, H. Gemmeke, C. Kaiser, J. Knaudt, N.V. Ruiter: 3D ultrasound computer tomography: update from a clinical study. In: SPIE Medical Imaging 2016. Proc. of SPIE Vol. 9790, 97900A.

[4] J.F. Greenleaf, R.C. Bahn: Clinical imaging with transmissive ultrasonic computerized tomography. IEEE Trans Biomed Imaging 28(2) (1981) 177-185.

[5] T. Hopp, M. Dietzel, P.A. Baltzer, P. Kreisel, W.A. Kaiser, H. Gemmeke, N.V. Ruiter: Automatic multimodal 2D/3D breast image registration using biomechnical FEM models and intensity-based optimization. Medical Image Analysis 17 (2013) 209-218.

[6] J.C. Bezdek: Pattern Recognition with Fuzzy Objective Function Algorithms, Kluwer Academic Publishers, Norwell, MA, USA (1981).

[7] C. Li, R. Huang, Z. Ding, J. Gatenby, D. Metaxas, J. Gore: A Level Set Method for Image Segmentation in the Presence of Intensity Inhomogeneities With Application to MRI. IEEE Transactions on Image Processing 20(7) (2011) 2007-2016.

[8] T.J. Carter, C. Tanner, D.J. Hawkes: Determining material properties of the breast for image-guided surgery. In: Proc. SPIE Medical Imaging 7261 (2009) 726124.

[9] Q. Fang, D. Boas: Tetrahedral mesh generation from volumetric binary and grayscale images. In: IEEE International Symposium on Biomedical Imaging: From Nano to Macro 2009 (2009) 1142-1145.

[10] A. Bower: Applied Mechanics of Solids, Taylor and Francis (2011).

[11] Dassault Systems Simulia Corp, ABAQUS Analysis User's Manual (2014).

[12] S. Kirkpatrick, C.D. Gelatt, M.P. Vecchi: Optimization by Simulated Annealing. Science 220(4598) (1983) 671-680.

[13] T. Hopp, N. Duric, N.V. Ruiter: Image fusion of Ultrasound Computer Tomography volumes with X-ray mammograms using a biomechanical model based 2D/3D registration. Computerized Medical Imaging and Graphics 40 (2015) 170-181.

[14] T. Hopp, R. Dapp, M. Zapf, E. Kretzek, H. Gemmeke, N.V. Ruiter: Registration of 3D Ultrasound computer Tomography and MRI for evaluation of tissue correspondences. In: SPIE Medical Imaging 2015. Proc. of SPIE Vol. 9419, 94190Q-1.

[15] E.A. Hauth, C. Stockamp, S. Maderwald, A. Mhler, R. Kimming, H. Jaeger, J. Barkhausen, M. Forsting: Evaluation of the three-time point method for diagnosis of breast lesions in contrast-enhanced MR mammography. Clinical Imaging 30(3) (2006) 160-165.

[16] N. Cristianini, J. Shawe-Taylor: An introduction to Support Vector Machines and other kernel-based learning methods. New York, NY, USA: Cambridge University Press 2000.